Antenna Tilt Design for Millimeter-Wave Beamspace MIMO Systems

Anzhong Hu

Wireless Personal Communications
An International Journal

ISSN 0929-6212
Volume 94
Number 3

Wireless Pers Commun (2017)
94:1701-1713
DOI 10.1007/s11277-016-3707-9

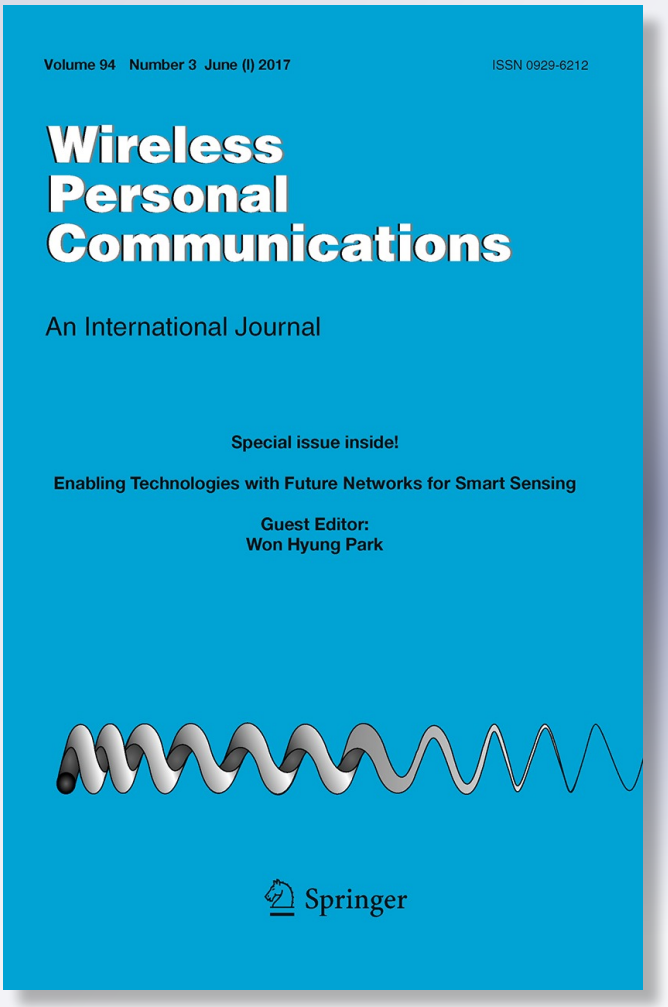

Springer

Your article is protected by copyright and all rights are held exclusively by Springer Science +Business Media New York. This e-offprint is for personal use only and shall not be self-archived in electronic repositories. If you wish to self-archive your article, please use the accepted manuscript version for posting on your own website. You may further deposit the accepted manuscript version in any repository, provided it is only made publicly available 12 months after official publication or later and provided acknowledgement is given to the original source of publication and a link is inserted to the published article on Springer's website. The link must be accompanied by the following text: "The final publication is available at link.springer.com".

Author's personal copy

Wireless Pers Commun (2017) 94:1701–1713
DOI 10.1007/s11277-016-3707-9

Antenna Tilt Design for Millimeter-Wave Beamspace MIMO Systems

Anzhong Hu[1]

Published online: 17 September 2016
© Springer Science+Business Media New York 2016

Abstract A joint design of the mechanical and the electrical tilts is proposed for millimeter-wave beamspace multiple-input multiple-output systems. Based on the correlation property of the array steering vector, the asymptotic sum rate is derived. In order to maximize the sum rate, the mechanical tilt is designed to maximize the expectations of the antenna gains. Moreover, the electrical tilt is dynamically adjusted to optimize the instantaneous antenna gains. As a result, the proposed joint design of two tilts can achieve higher sum rate than the designs of one tilt, which is confirmed by the simulation results.

Keywords Millimeter-wave · Beamspace multiple-input multiple-output (B-MIMO) · Antenna tilt · Uniform rectangular array (URA) · Direction-of-arrival (DOA)

1 Introduction

Millimeter-wave (mm-wave) beamspace multiple-input multiple-output (B-MIMO) systems, which operate from 30 GHz to 300 GHz, are introduced to achieve high gain of spectral efficiency with low complexity [1, 2]. However, antenna tilt is fixed in these systems, which means the degrees of freedom in the vertical dimension are not fully exploited. Recently, a few antenna tilting schemes are proposed for conventional MIMO systems [3–5], but only the mechanical tilt or the electrical tilt is designed. In this letter, a joint design of the two tilts is proposed for mm-wave B-MIMO systems. First, the partial beams are selected according to the spatial frequencies of the beams and the spatial frequencies of the mobile stations (MSs). Then, the asymptotic sum rate in the limit of the access point (AP) antennas, i.e., $\lim_{N\to\infty} R$, is derived, where N is the number of the AP antennas, and R is the sum rate. As the sum rate increases with the increase of the antenna

✉ Anzhong Hu
huaz@hdu.edu.cn

[1] School of Communication Engineering, Hangzhou Dianzi University, Hangzhou 310018, China

Author's personal copy

gains, the optimal mechanical tilt which maximizes the expectations of the antenna gains is derived. In addition, the electrical tilt is dynamically adjusted to optimize the instantaneous antenna gains. Compared with the designs of one tilt, the proposed design is able to achieve better performance.

Notations: Lower-case boldface symbols denote vectors, upper-case boldface symbols denote matrices; $\mathbf{I}_K$ represents the $K \times K$ identity matrix; $(\cdot)^H$, tr$(\cdot)$, and $\mathbb{E}\{\cdot\}$ denote the conjugate transpose, the trace, and the expectation, respectively; $||\cdot||$ is the Euclidean norm of a vector; $[\cdot]_j$ is the j-th element of a vector or the j-th column of a matrix; $[\cdot]_{j,l}$ is the element in the j-th row and the l-th column of a matrix; and i is the imaginary unit.

2 mm-Wave System Model

2.1 An mm-Wave Scenario

A schematic illustration of the investigated system is shown in Fig. 1. The AP is equipped with a uniform rectangular array (URA), and serves K single antenna MSs. The system works at mm-wave and adopts time division duplex (TDD) mode. The number of antennas of the URA is $N = N_{\text{az}}N_{\text{el}}$, where N_{az} and N_{el} are the numbers of the antennas in the azimuth and elevation directions of the URA, respectively.

The focus of this letter is downlink transmission, in which the AP transmits signals to the MSs. The received signal vector at the K MSs is

$$\mathbf{r} = \mathbf{H}^H\mathbf{G}\mathbf{s} + \mathbf{n} \in \mathbb{C}^{K\times 1}, \tag{1}$$

where $\mathbf{H} \in \mathbb{C}^{N\times K}$ is the downlink channel matrix, $\mathbf{G} \in \mathbb{C}^{N\times K}$ is precoding matrix, $\mathbf{s} \in \mathbb{C}^{K\times 1}$ is the symbol vector, and $\mathbf{n} \in \mathbb{C}^{K\times 1}$ is the noise vector of zero-mean Gaussian variables with covariance matrix $\sigma_{\text{n}}^2\mathbf{I}_K$. As can be seen, $[\mathbf{r}]_k$ is the received symbol at the k-th MS, the k-th row of $\mathbf{H}$ is the channel vector from the AP to the k-th MS, $[\mathbf{s}]_k$ is the transmitted symbol for the k-th MS, and $[\mathbf{n}]_k$ is the received noise at the k-th MS. The correlation matrix of $\mathbf{s}$ is $\mathbb{E}\{\mathbf{s}\mathbf{s}^H\} = \Lambda_{\text{s}} \in \mathbb{R}^{K\times K}$, which is a diagonal matrix, and the power satisfies $\mathbb{E}\{||\mathbf{G}\mathbf{s}||^2\} = \text{tr}(\mathbf{G}\Lambda_{\text{s}}\mathbf{G}^H) \le \rho/N$,where ρ is the constraint of the transmission power of the AP. Because the propagation at mm-wave is highly directional, it is assumed

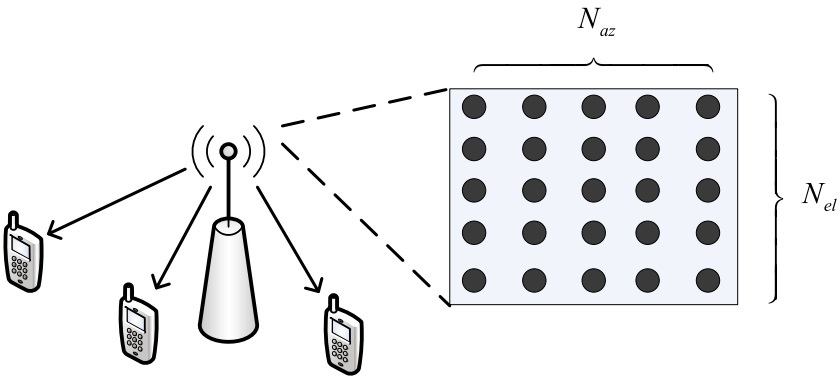

Fig. 1 A schematic illustration of the investigated system

Author's personal copy

that there is only line-of-sight transmission. Accordingly, the channel vector of the k-th MS is expressed as [2]

$$[\mathbf{H}]_k = \beta_k \mathbf{a}(\theta_k^{\text{az}}, \theta_k^{\text{el}}), \tag{2}$$

where β_k is the complex path loss, $\mathbf{a}(\theta_k^{\text{az}}, \theta_k^{\text{el}}) \in \mathbb{C}^{N\times 1}$ is the array steering vector; θ_k^{az} and θ_k^{el} are the azimuth direction-of-arrival (DOA) and the elevation DOA of the k-th MS, respectively.

2.2 The Role of the Mechanical and Electrical Tilts

More explicitly, an illustration of the DOAs is shown in Fig. 2, in which the axes and the AP are located in the same way as [2]. As can be seen in Fig. 2, in the considered system topology, the center of the URA is at the origin of the axes, and the URA plane is orthogonal to the x axis. The mechanical tilt of the URA is the angle between the z axis and the URA plane. When the mechanical tilt of the URA is zero, the URA is in the y-z plane. When the mechanical tilt of the URA is positive/negative, the URA is turned in the direction from the x axis to the z axis/from the z axis to the x axis. In the example shown in Fig. 2, the URA is turned in the direction from the z axis to the x axis, and the mechanical tilt of the URA is negative, which is ϕ_{mec} in the figure. Thus, $-\phi_{\text{mec}}$ is positive and is also the angle between the x axis and the normal of the URA plane in Fig. 2.

In Fig. 2, θ_k^{az} is the azimuth DOA, which is the angle from the normal of the URA plane to the projection from the line connecting the MS and the origin to the plane in the y axis and the normal of the URA plane, and is positive/negative when the MS is above/below the x-z plane; θ_k^{el} is the elevation DOA, which is the angle from the line connecting the MS and the origin to the plane in the y axis and the normal of the URA plane, and is positive/negative when the MS is above/below that plane. Accordingly, the DOAs are defined as [2]

$$\sin\theta_k^{\text{az}} = \frac{r_k \sin\eta_k}{\sqrt{(r_k\cos\eta_k\cos\phi_{\text{mec}} - h\sin\phi_{\text{mec}})^2 + (r_k\sin\eta_k)^2}} \tag{3}$$

$$\sin\theta_k^{\text{el}} = \frac{-r_k\cos\eta_k\sin\phi_{\text{mec}} - h\cos\phi_{\text{mec}}}{\sqrt{r_k^2 + h^2}}, \tag{4}$$

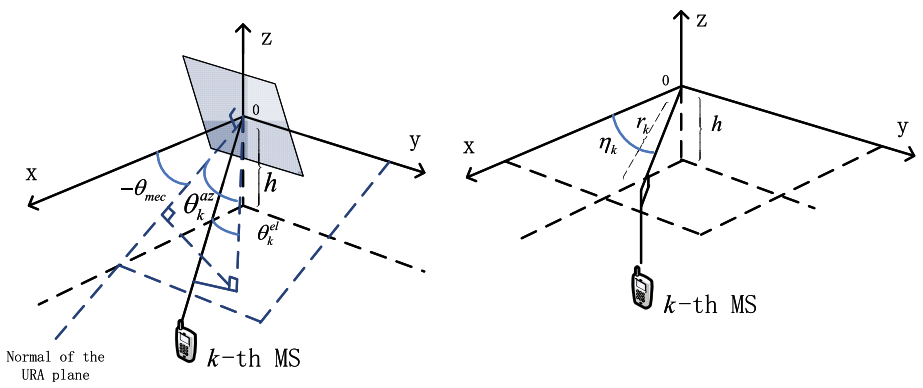

Fig. 2 An illustration of the system topology and the DOAs

Author's personal copy

where ϕ_{mec} is the mechanical tilt of the URA, r_k and η_k are the polar coordinates of the k-th MS in the x-y plane; h is the distance between the MSs and the x-y plane, i.e., the MSs are in an plane that is parallel to the x-y plane. The derivation of Eqs. (3) and (4) from [2] are shown in the Appendix.

The phase of the path loss is a uniformly distributed random variable in the interval $[0, 2\pi]$, and the amplitude of the path loss is modeled with the Friis formula as [6]

$$|\beta_k|^2 = \frac{D(\theta_k^{\text{az}}, \theta_k^{\text{el}}, \phi_{\text{e}})\lambda^2}{16\pi^2(r_k^2 + h^2)}, \tag{5}$$

where ϕ_{e} is the electrical tilt of the antenna, and is negative when tilting below the x-y plane, is positive when tilting above the x-y plane; λ is the wavelength, $D(\theta_k^{\text{az}}, \theta_k^{\text{el}}, \phi_{\text{e}})$ is the antenna directivity defined as [7]

$$\begin{aligned} D(\theta_k^{\text{az}}, \theta_k^{\text{el}}) &= 10^{-0.1\min\left(-A_{\text{az}}(\theta_k^{\text{az}}) - A_{\text{el}}(\theta_k^{\text{el}}), SLL\right)} \\ A_{\text{az}}(\theta_k^{\text{az}}) &= -\min\left(12\left(\frac{\theta_k^{\text{az}}}{\theta_{\text{3dB}}^{\text{az}}}\right)^2, SLL_{\text{az}}\right) \\ A_{\text{el}}(\theta_k^{\text{el}}) &= -\min\left(12\left(\frac{\theta_k^{\text{el}} - \phi_{\text{e}}}{\theta_{\text{3dB}}^{\text{el}}}\right)^2, SLL_{\text{el}}\right), \end{aligned} \tag{6}$$

where SLL, SLL_{az}, and SLL_{el} are the overall, the azimuth, and the elevation side lobe levels, respectively; $\theta_{\text{3dB}}^{\text{az}}$ and $\theta_{\text{3dB}}^{\text{el}}$ are the half-power beamwidth (HPBW) in the azimuth and the elevation antenna radiation pattern. The steering vector in (2) is defined as

$$\begin{aligned} [\mathbf{a}(\theta^{\text{az}}, \theta^{\text{el}})]_n = {} & e^{i\pi(n_{\text{az}} - 0.5(N_{\text{az}}-1))\cos\theta^{\text{el}}\sin\theta^{\text{az}}} \\ & \times e^{i\pi(n_{\text{el}} - 0.5(N_{\text{el}}-1))\sin\theta^{\text{el}}}, \end{aligned} \tag{7}$$

where $n_{\text{az}} = 0, 1, \ldots, N_{\text{az}} - 1$, $n_{\text{el}} = 0, 1, \ldots, N_{\text{el}} - 1$, and $n = n_{\text{el}}N_{\text{az}} + n_{\text{az}} + 1$. Moreover, $\cos\theta^{\text{el}}\sin\theta^{\text{az}}$ and $\sin\theta^{\text{el}}$ are termed as spatial frequencies. According to the idea of B-MIMO, the steering vector can be utilized to construct a unitary matrix, $\mathbf{U} \in \mathbb{C}^{N\times N}$, where

$$[\mathbf{U}]_m = \mathbf{a}(\tilde{\theta}_m^{\text{az}}, \tilde{\theta}_m^{\text{el}})/\sqrt{N}, \tag{8}$$

and the spatial frequencies satisfy $\cos\tilde{\theta}_m^{\text{el}}\sin\tilde{\theta}_m^{\text{az}} = -1 + 2m_{\text{az}}/N_{\text{az}}$, $\sin\tilde{\theta}_m^{\text{el}} = -1 + 2m_{\text{el}}/N_{\text{el}}$, $m = (m_{\text{el}} - 1)N_{\text{az}} + m_{\text{az}}$, $m_{\text{az}} = 1, 2, \ldots, N_{\text{az}}$, and $m_{\text{el}} = 1, 2, \ldots, N_{\text{el}}$. Then, $\mathbf{U}$ is employed as a beamforming matrix, and the columns of $\mathbf{U}$ are termed as the orthogonal beams in the space. In order to reduce complexity, N_{b} beams are selected for beamforming, and the beamforming matrix is $\mathbf{U}_{\text{b}} \in \mathbb{C}^{N\times N_{\text{b}}}$.

2.3 Beamspace Signal Processing

Because of the channel reciprocity of the TDD systems, the transmission process is as follows.

- The MSs transmit orthogonal pilots and the AP estimates the spatial frequencies.
- The AP selects N_{b} beams from the N beams, N_{b}/K beams are selected for each MS according to the spatial frequencies of the MSs and the spatial frequencies of the

Author's personal copy

beams. More specifically, calculate the differences between the spatial frequencies of the beams and the spatial frequency of each MS, and the beams that have been selected for other MSs are not included in the calculation; the N_b/K beams corresponding to the smallest differences are selected for that MS. Note that this selection method is simpler than the conventional methods which utilize the correlation of the channel vectors and the beams.

- The AP transmits data symbols to the MSs in the selected beamspace.

Assuming perfect knowledge of the channels is available at the AP, and minimum mean square error precoding is applied, i.e., $\mathbf{G} = \alpha\mathbf{F}$, where

$$\mathbf{F} = \mathbf{U}_b\mathbf{H}_b(\mathbf{H}_b^H\mathbf{H}_b + (\sigma_n^2 KN/\rho)\mathbf{I}_K)^{-1} \in \mathbb{C}^{N\times K}, \tag{9}$$

$$\mathbf{H}_b = \mathbf{U}_b^H\mathbf{H} \in \mathbb{C}^{N_b\times K}, \tag{10}$$

and $\alpha = \sqrt{\rho/(N\mathrm{tr}(\mathbf{F}\Lambda_s\mathbf{F}^H))}$. Then, the received signal in (1) can be re-expressed as $\mathbf{r} = \alpha\mathbf{A}\mathbf{s} + \mathbf{n}$, where

$$\mathbf{A} = \mathbf{H}^H\mathbf{F} = \mathbf{H}_b^H\mathbf{H}_b(\mathbf{H}_b^H\mathbf{H}_b + (\sigma_n^2 KN/\rho)\mathbf{I}_K)^{-1} \in \mathbb{C}^{K\times K}. \tag{11}$$

Consequently, the sum rate can be expressed as

$$R = \sum_{k=1}^{K}\log_2\left(1 + \frac{\alpha^2\left|[\mathbf{A}]_{k,k}\right|^2[\Lambda_s]_{k,k}}{\alpha^2\sum_{\substack{k'=1\\k'\neq k}}^{K}\left(\left|[\mathbf{A}]_{k,k'}\right|^2[\Lambda_s]_{k',k'}\right) + \sigma_n^2}\right). \tag{12}$$

The detailed derivation of the sum rate is shown in the Appendix.

3 Joint Design of the Mechanical and Electrical Tilts

3.1 Analysis of Sum Rate in the Limit of AP Antennas

With the system model presented, the mechanical and the electrical tilts are designed here to maximize the sum rate. According to the expression of the array steering vector in (7) and the definition of the beams, it can be seen that

$$\lim_{N_{az},N_{el}\to\infty}\frac{1}{N}\left|\mathbf{a}^H(\tilde{\theta}_m^{az},\tilde{\theta}_m^{el})\mathbf{a}(\theta_k^{az},\theta_k^{el})\right| = c_{k,m} \tag{13}$$

when $\lim_{N_{az}\to\infty} d_{k,m}^{az}N_{az}$ and $\lim_{N_{el}\to\infty} d_{k,m}^{el}N_{el}$ are finite numbers, where

$$c_{k,m} = \frac{\left|1 - e^{i\pi N_{az}d_{k,m}^{az}}\right|\left|1 - e^{i\pi N_{el}d_{k,m}^{el}}\right|}{\pi^2 N\left|d_{k,m}^{az}d_{k,m}^{el}\right|} \tag{14}$$

is the correlation of the array steering vector and the beam vector,

$$d_{k,m}^{az} = \cos\theta_k^{el}\sin\theta_k^{az} - \cos\tilde{\theta}_m^{el}\sin\tilde{\theta}_m^{az}, \tag{15}$$

$$d_{k,m}^{el} = \sin\theta_k^{el} - \sin\tilde{\theta}_m^{el} \tag{16}$$

Author's personal copy

are the differences of the spatial frequencies. The derivation of Eq. (14) is shown in the Appendix. Additionally, there is

$$\lim_{N_{\mathrm{az}},N_{\mathrm{el}}\to\infty} \mathbf{a}^H(\tilde{\theta}_m^{\mathrm{az}},\tilde{\theta}_m^{\mathrm{el}})\mathbf{a}(\theta_k^{\mathrm{az}},\theta_k^{\mathrm{el}})/N = 0 \tag{17}$$

when $\lim_{N_{\mathrm{az}}\to\infty} d_{k,m}^{\mathrm{az}} N_{\mathrm{az}}$ or $\lim_{N_{\mathrm{el}}\to\infty} d_{k,m}^{\mathrm{el}} N_{\mathrm{el}}$ is infinitely large. Among all the spatial frequencies of the selected beams, only the spatial frequencies of the beams selected for an MS approach the spatial frequencies of that MS. Thus, the elements of $\lim_{N_{\mathrm{az}},N_{\mathrm{el}}\to\infty} \mathbf{U}_{\mathrm{b}}^H[\mathbf{H}]_k/\sqrt{N}$ are zeros except those correspond to the selected beams of the k-th MS. Consequently, $\mathbf{H}_{\mathrm{b}}^H\mathbf{H}_{\mathrm{b}}/N$ tends to be a diagonal matrix as N_{az} and N_{el} tend to infinity, and

$$\lim_{N_{\mathrm{az}},N_{\mathrm{el}}\to\infty} \frac{[\mathbf{H}_{\mathrm{b}}^H\mathbf{H}_{\mathrm{b}}]_{k,k}}{N} = |\beta_k|^2 \sum_{m\in\mathcal{B}_k} |c_{k,m}|^2, \tag{18}$$

where $\mathcal{B}_k$ is the set of beam indices that are selected for the k-th MS. Then, the asymptotic sum rate in the limits of N_{az} and N_{el} can be written as

$$\tilde{R} = \sum_{k=1}^{K} \log_2\left(1 + \frac{\rho\left|\left[\Lambda_{\mathrm{b}}\left(\Lambda_{\mathrm{b}} + \left(\sigma_{\mathrm{n}}^2 K/\rho\right)\mathbf{I}_K\right)^{-1}\right]_{k,k}\right|^2 [\Lambda_{\mathrm{s}}]_{k,k}}{\sigma_{\mathrm{n}}^2 \mathrm{tr}\left(\left(\Lambda_{\mathrm{b}} + \left(\sigma_{\mathrm{n}}^2 K/\rho\right)\mathbf{I}_K\right)^{-2}\Lambda_{\mathrm{b}}\Lambda_{\mathrm{s}}\right)}\right), \tag{19}$$

where $\Lambda_{\mathrm{b}} \in \mathbb{R}^{K\times K}$ is a diagonal matrix with the k-th diagonal element being $[\Lambda_{\mathrm{b}}]_{k,k} = |\beta_k|^2 \sum_{m\in\mathcal{B}_k} |c_{k,m}|^2$. The derivation of the asymptotic sum rate is shown in the Appendix.

3.2 Design of the Two Tilts for Maximizing the Sum Rate

It is easy to find that $\tilde{R}$ increases with the increase of $|\beta_k|^2$. From (5) and (6), it can be seen that $|\beta_k|^2$ is mainly determined by θ_k^{el} and ϕ_{e} when θ_k^{az} is much smaller than $\theta_{3\mathrm{dB}}^{\mathrm{az}}$, which is usually the case. Moreover, given any electrical tilt, the expectation of $|\beta_k|^2$ is maximized when the variance of θ_k^{el} is minimized. Based on these facts, the two tilts are jointly designed as follows. First, the mechanical tilt is designed to minimize the variance of θ_k^{el}. According to the definition of the elevation DOA in (4), it is easy to verify that the covariance of $\sin(\theta_k^{\mathrm{el}})$ is minimized when $\phi_{\mathrm{mec}} = 0$. Additionally, with Taylor series expansion, it can be found that the covariance of $\sin(\theta_k^{\mathrm{el}})$ is approximately proportional to the covariance of θ_k^{el}. Therefore, the optimal mechanical tilt is $\phi_{\mathrm{mec}} = 0$. Then, the electrical tilt is adjusted to optimize the instantaneous antenna gains with the object, $\arg\max_{\phi_{\mathrm{e}}} \tilde{R}$, where ϕ_{e} is in the same range as the elevation DOA, $\theta_k^{\mathrm{el}}, \forall k$ in (4). The design steps are as follows.

- Calculate the range of the elevation DOA given the optimal mechanical tilt.
- Sample the range of the elevation DOA equally, set the electrical tilt to each sampled value and calculate the corresponding asymptotic sum rate.
- Set the electrical tilt to the sample point with the highest sum rate.

Note that the mechanical tilt is fixed as long as it is designed since it statistically maximizes the antenna gains. On the contrary, the electrical tilt is adjusted dynamically as it instantaneously optimizes the antenna gains.

Author's personal copy

4 Results

The main simulation parameters are set as $N_{az} = 16$, $N_{el} = 76$, $K = 100$, $h = 10$ m, the operating frequency is 80 GHz, the cell is a sector of 120° with cell radius in the range [10, 100] m, $N_b = 4K$, $\theta_{3dB}^{az} = 70°$, $\theta_{3dB}^{el} = 7°$, $SLL = 25$ dB, $SLL_{az} = 25$ dB, and $SLL_{el} = 20$ dB, $\Lambda_s = (1/K)\mathbf{I}_K$. The transmit signal-to-noise ratio (SNR) is 112 dB, where the SNR is calculated with $\rho/(N\sigma_n^2)$.

The spectral efficiencies versus the transmit SNR are compared in Fig. 3. With the fixed mechanical tilt, the array points to the center of the cell area. With the dynamic electrical tilt, the electrical tilt is adjusted to maximize the spectral efficiency with the fixed mechanical tilt which is directed to the center of the cell area. It can be seen that the proposed antenna tilt design can achieve higher spectral efficiency than the other approaches. The results verify that the design of two tilts is able to exploit the spatial dimension more efficiently in mm-wave B-MIMO systems.

The spectral efficiencies versus the number of MSs K are illustrated in Fig. 4. When the number of MSs increases, the multiplexing gain increases, which results into the increase of the spectral efficiency. This corresponds to the increase of the spectral efficiency in Fig. 4. However, as the number of MSs increases, the interference to each MS also increases, which leads to a decrease of the increasing rate of the spectral efficiency. This is verified by the fact that the curves in Fig. 4 tend to be flat as K increases. Most importantly, the proposed antenna tilt design is always of higher spectral efficiency than the other approaches.

The spectral efficiencies versus the maximal radius of the cell are illustrated in Fig. 5. As the maximal cell radius increases, the path loss increases, which causes a degradation of the spectral efficiency. This result can be seen in Fig. 5. Additionally, when the cell radius increases, the steering range of the electrical tilt increases, which makes the tilt designs with adjustable electrical tilt of higher spectral efficiencies than the fixed mechanical tilt. As can be seen in Fig. 5, the performance improvement of the proposed antenna tilt design is obvious.

The spectral efficiencies versus HPBW in the elevation pattern θ_{3dB}^{el} are illustrated in Fig. 6. As the HPBW increases, the selected beams are of higher antenna gain, which

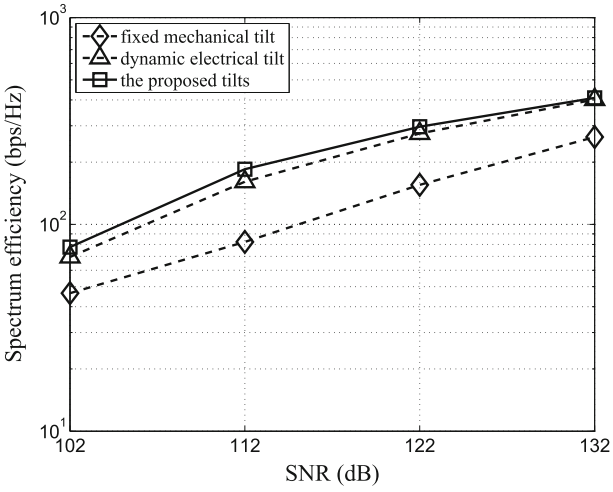

Fig. 3 The spectral efficiencies versus the SNR

Author's personal copy

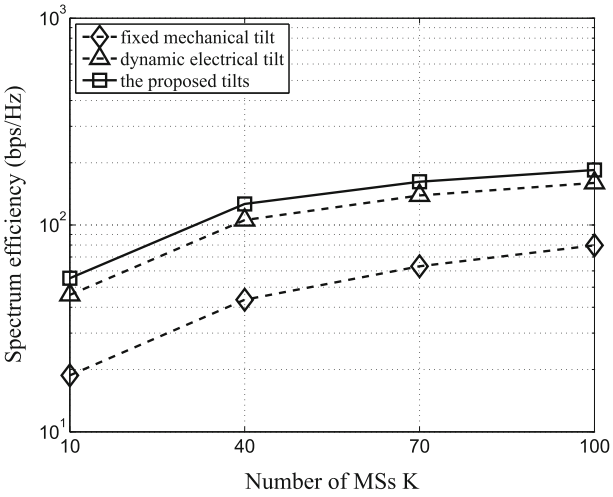

Fig. 4 The spectral efficiencies versus the number MSs K

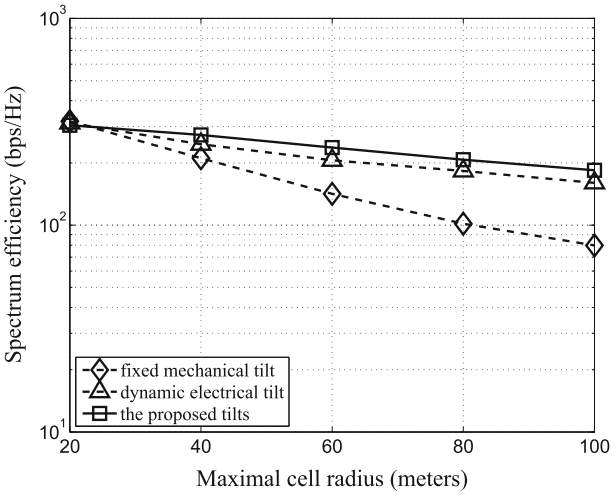

Fig. 5 The spectral efficiencies versus the maximal radius of the cell

causes the increase of the spectral efficiency. This result can be seen in Fig. 6. Moreover, the proposed antenna tilt design is of higher spectral efficiency than other tilt designs. This result demonstrates that the proposed tilts are suitable for a wide range of the HPBW in the elevation pattern.

5 Conclusion

According to the transmission property of mm-wave B-MIMO, the spatial frequencies instead of the channel response vectors are utilized for selecting the beams with low complexity. Then, the sum rate is derived and further simplified based on the limiting property of the array steering vector. In order to maximize the sum rate, the mechanical tilt is designed to maximize the expectations of the antenna gains. Additionally, the electrical

Author's personal copy

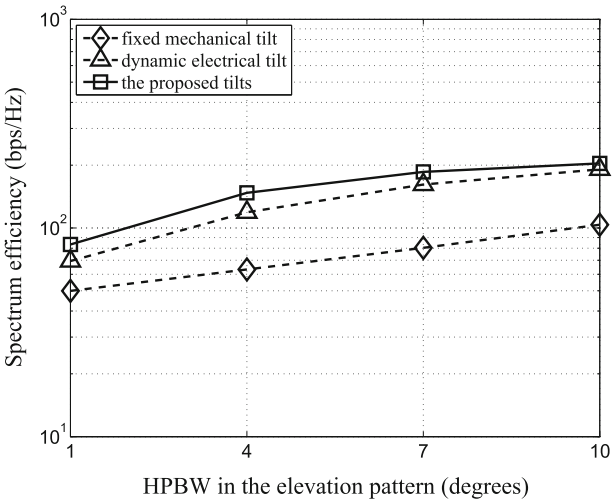

Fig. 6 The spectral efficiencies versus the HPBW in the elevation pattern $\theta_{3\text{dB}}^{\text{el}}$

tilt is adjusted dynamically to optimize the instantaneous antenna gains based on the sum rate expression. As the mechanical tilt is fixed after the design and the sum rate expression is simplified, the tilt design is feasible for implementation. Moreover, the design of two tilts results in performance improvement in comparison to the designs of one tilt.

Acknowledgments The author would like to thank Editor in Chief R. Prasad and the two anonymous reviewers for their valuable suggestions to refine the paper. This research was supported by Zhejiang Provincial Natural Science Foundation of China under Grant No. LQ16F010007 and Scientific Research Starting Foundation of Hangzhou Dianzi University under Grant No. KYS085614054.

Appendix

Derivation of Equations (3) and (4)

In [2], equations (6) and (7) are written as

$$\theta_k^{\text{az}} = \frac{1}{2}\frac{R_k \sin\eta_k}{\sqrt{\left(R_k\cos\eta_k\cos\psi + h\sin\psi\right)^2 + R_k^2\sin^2\eta_k}}$$

$$\theta_k^{\text{el}} = \frac{1}{2}\frac{R_k\cos\eta_k\sin\psi - h\cos\psi}{\sqrt{R_k^2\cos\eta_k^2 + h^2}}.$$

In fact, the definitions of the symbols are different in this paper and [2]. For θ_k^{az}, θ_k^{el}, R_k, and ψ in [2], the corresponding symbols or equations of the same value are $0.5\sin\theta_k^{\text{az}}$, $0.5\sin\theta_k^{\text{el}}$, r_k, and $-\phi_{\text{mec}}$, in this paper, respectively. By replacing the symbols of [2] with the symbols of this paper, Eqs. (6) turns into Eq. (3) here. For Eq. (7) in [2], there is a typo error, i.e., $R_k^2\cos\eta_k^2$ should be R_k^2. The reason is that the elevation angle is calculated with the distance between the MS and the origin, which is $\sqrt{R_k^2 + h^2}$ rather than $\sqrt{R_k^2\cos\eta_k^2 + h^2}$. After this

Author's personal copy

little modification and replacing the symbols of [2] with the symbols of this paper, Eq. (4) in this paper can be derived.

Derivation of the Sum Rate in (12)

According to the expression of the received signal vector at the K MSs, $\mathbf{r} = \alpha\mathbf{A}\mathbf{s} + \mathbf{n}$, which is stated below (11), it can be seen that the received signal at the k-th MS is $[\mathbf{r}]_k = \alpha \sum_{k'=1}^{K} [\mathbf{A}]_{k,k'}[\mathbf{s}]_{k'} + [\mathbf{n}]_k$. The desired signal is $\alpha[\mathbf{A}]_{k,k}[\mathbf{s}]_k$, and the other parts of the received signal are interference and noise, which are $\alpha \sum_{\substack{k'=1 \\ k' \neq k}}^{K} [\mathbf{A}]_{k,k'}[\mathbf{s}]_{k'}$ and $[\mathbf{n}]_k$, respectively. Since the correlation of $\mathbf{s}$ is $\mathbb{E}\{\mathbf{s}\mathbf{s}^H\} = \Lambda_\mathrm{s}$ and the correlation of the noise $\mathbf{n}$ is $\sigma_\mathrm{n}^2\mathbf{I}_K$, the signal power at the k-th MS is $\alpha^2 |[\mathbf{A}]_{k,k}|^2 [\Lambda_\mathrm{s}]_{k,k}$, the interference power at the k-th MS is $\alpha^2 \sum_{\substack{k'=1 \\ k' \neq k}}^{K} |[\mathbf{A}]_{k,k'}|^2 [\Lambda_\mathrm{s}]_{k,k'}$, and the noise power at the k-th MS is σ_n^2. As a result, the signal-to-interference-plus-noise ratio at the the k-th MS is

$$\gamma_k = \frac{\alpha^2 |[\mathbf{A}]_{k,k}|^2 [\Lambda_\mathrm{s}]_{k,k}}{\alpha^2 \sum_{\substack{k'=1 \\ k' \neq k}}^{K} |[\mathbf{A}]_{k,k'}|^2 [\Lambda_\mathrm{s}]_{k,k'} + \sigma_\mathrm{n}^2}.$$

Since the sum rate of the system is $R = \sum_{k=1}^{K} \log_2(1 + \gamma_k)$, the sum rate can be written as

$$R = \sum_{k=1}^{K} \log_2 \left(1 + \frac{\alpha^2 \left| [\mathbf{A}]_{k,k} \right|^2 [\Lambda_\mathrm{s}]_{k,k}}{\alpha^2 \sum_{\substack{k'=1 \\ k' \neq k}}^{K} \left(\left| [\mathbf{A}]_{k,k'} \right|^2 [\Lambda_\mathrm{s}]_{k',k'} \right) + \sigma_\mathrm{n}^2} \right),$$

which is exactly Eq. (12).

Derivation of Equation (14)

According to the expression of the array steering vector in (7), the definition of the beams in (8) and the definitions in (15) and (16), we have

$$\begin{aligned}
&\left| \mathbf{a}^H(\tilde{\theta}_m^{\mathrm{az}}, \tilde{\theta}_m^{\mathrm{el}}) \mathbf{a}(\theta_k^{\mathrm{az}}, \theta_k^{\mathrm{el}}) \right| \\
&= \left| \sum_{n_{\mathrm{az}}=0}^{N_{\mathrm{az}}-1} \sum_{n_{\mathrm{el}}=0}^{N_{\mathrm{el}}-1} e^{i\pi(n_{\mathrm{az}} - 0.5(N_{\mathrm{az}}-1))\left(\cos\theta^{\mathrm{el}} \sin\theta^{\mathrm{az}} - \cos\tilde{\theta}_m^{\mathrm{el}} \sin\tilde{\theta}_m^{\mathrm{az}}\right)} \right. \\
&\quad \left. \times e^{i\pi(n_{\mathrm{el}} - 0.5(N_{\mathrm{el}}-1))\left(\sin\theta^{\mathrm{el}} - \sin\tilde{\theta}_m^{\mathrm{el}}\right)} \right| \\
&= \left| \sum_{n_{\mathrm{az}}=0}^{N_{\mathrm{az}}-1} \sum_{n_{\mathrm{el}}=0}^{N_{\mathrm{el}}-1} e^{i\pi n_{\mathrm{az}} d_{k,m}^{\mathrm{az}}} e^{i\pi n_{\mathrm{el}} d_{k,m}^{\mathrm{el}}} \right| \\
&= \left| \frac{1 - e^{i\pi N_{\mathrm{az}} d_{k,m}^{\mathrm{az}}}}{1 - e^{i\pi d_{k,m}^{\mathrm{az}}}} \frac{1 - e^{i\pi N_{\mathrm{el}} d_{k,m}^{\mathrm{el}}}}{1 - e^{i\pi d_{k,m}^{\mathrm{el}}}} \right|.
\end{aligned}$$

In the limit that $N_{\mathrm{az}}, N_{\mathrm{el}} \to \infty$ while $\lim_{N_{\mathrm{az}} \to \infty} d_{k,m}^{\mathrm{az}} N_{\mathrm{az}}$ and $\lim_{N_{\mathrm{el}} \to \infty} d_{k,m}^{\mathrm{el}} N_{\mathrm{el}}$ are finite numbers, which means $d_{k,m}^{\mathrm{az}}, d_{k,m}^{\mathrm{el}} \to 0$, we have

Author's personal copy

$$\begin{aligned}
&\lim_{N_{\mathrm{az}},N_{\mathrm{el}}\to\infty}\frac{1}{N}\left|\mathbf{a}^H(\tilde{\theta}_m^{\mathrm{az}},\tilde{\theta}_m^{\mathrm{el}})\mathbf{a}(\theta_k^{\mathrm{az}},\theta_k^{\mathrm{el}})\right| \\
&=\lim_{N_{\mathrm{az}},N_{\mathrm{el}}\to\infty}\left|\frac{1}{N_{\mathrm{az}}}\frac{1-e^{i\pi N_{\mathrm{az}}d_{k,m}^{\mathrm{az}}}}{1-e^{i\pi d_{k,m}^{\mathrm{az}}}}\frac{1}{N_{\mathrm{el}}}\frac{1-e^{i\pi N_{\mathrm{el}}d_{k,m}^{\mathrm{el}}}}{1-e^{i\pi d_{k,m}^{\mathrm{el}}}}\right| \\
&=\lim_{N_{\mathrm{az}},N_{\mathrm{el}}\to\infty}\left|\frac{d_{k,m}^{\mathrm{az}}}{1-e^{i\pi d_{k,m}^{\mathrm{az}}}}\frac{1-e^{i\pi N_{\mathrm{az}}d_{k,m}^{\mathrm{az}}}}{N_{\mathrm{az}}d_{k,m}^{\mathrm{az}}}\frac{d_{k,m}^{\mathrm{el}}}{1-e^{i\pi d_{k,m}^{\mathrm{el}}}}\frac{1-e^{i\pi N_{\mathrm{el}}d_{k,m}^{\mathrm{el}}}}{N_{\mathrm{el}}d_{k,m}^{\mathrm{el}}}\right| \\
&=\left|\frac{1}{\pi^2}\frac{1-e^{i\pi N_{\mathrm{az}}d_{k,m}^{\mathrm{az}}}}{N_{\mathrm{az}}d_{k,m}^{\mathrm{az}}}\frac{1-e^{i\pi N_{\mathrm{el}}d_{k,m}^{\mathrm{el}}}}{N_{\mathrm{el}}d_{k,m}^{\mathrm{el}}}\right| \\
&=\frac{\left|1-e^{i\pi N_{\mathrm{az}}d_{k,m}^{\mathrm{az}}}\right|\left|1-e^{i\pi N_{\mathrm{el}}d_{k,m}^{\mathrm{el}}}\right|}{\pi^2 N\left|d_{k,m}^{\mathrm{az}}d_{k,m}^{\mathrm{el}}\right|},
\end{aligned}$$

which is $c_{k,m}$ in (14). In the derivation of the third equation, the limiting property

$$\lim_{d_{k,m}^{\mathrm{az}}\to 0}\left|\frac{d_{k,m}^{\mathrm{az}}}{1-e^{i\pi d_{k,m}^{\mathrm{az}}}}\right|=\left|\frac{1}{-i\pi}\right|=\frac{1}{\pi}$$

is employed.

Derivation of Asymptotic Sum Rate in (19)

According to the property of $\mathbf{H}_{\mathrm{b}}^H\mathbf{H}_{\mathrm{b}}$ above (18), we know that $\mathbf{H}_{\mathrm{b}}^H\mathbf{H}_{\mathrm{b}}/N$ is a diagonal matrix in the limit $N_{\mathrm{az}},N_{\mathrm{el}}\to\infty$. Moreover, equation (18) shows the limiting expression of each diagonal element of $\mathbf{H}_{\mathrm{b}}^H\mathbf{H}_{\mathrm{b}}/N$, which is exactly the expression of the corresponding diagonal element of Λ_{b} given below (19). Thus, we have

$$\lim_{N_{\mathrm{az}},N_{\mathrm{el}}\to\infty}\frac{1}{N}\mathbf{H}_{\mathrm{b}}^H\mathbf{H}_{\mathrm{b}}=\Lambda_{\mathrm{b}}.$$

Then, according to the definition of $\mathbf{A}$ in (11), we have

$$\begin{aligned}
\lim_{N_{\mathrm{az}},N_{\mathrm{el}}\to\infty}\mathbf{A}&=\frac{\mathbf{H}_{\mathrm{b}}^H\mathbf{H}_{\mathrm{b}}}{N}\left(\frac{\mathbf{H}_{\mathrm{b}}^H\mathbf{H}_{\mathrm{b}}}{N}+\frac{\sigma_{\mathrm{n}}^2K}{\rho}\mathbf{I}_K\right)^{-1} \\
&=\Lambda_{\mathrm{b}}(\Lambda_{\mathrm{b}}+\frac{\sigma_{\mathrm{n}}^2K}{\rho}\mathbf{I}_K)^{-1}.
\end{aligned}$$

Then, according to the definition of α below (10), the definition of $\mathbf{F}$ in (9), and the property that $\mathbf{U}_{\mathrm{b}}^H\mathbf{U}_{\mathrm{b}}=\mathbf{I}_{N_{\mathrm{b}}}$, we have

Author's personal copy

$$
\begin{aligned}
&\lim_{N_{\mathrm{az}},N_{\mathrm{el}}\to\infty}\alpha^2\\
&=\lim_{N_{\mathrm{az}},N_{\mathrm{el}}\to\infty}\frac{\rho}{N\mathrm{tr}(\mathbf{F}\Lambda_{\mathrm{s}}\mathbf{F}^H)}\\
&=\lim_{N_{\mathrm{az}},N_{\mathrm{el}}\to\infty}\frac{\rho}{N\mathrm{tr}(\Lambda_{\mathrm{s}}\mathbf{F}^H\mathbf{F})}\\
&=\lim_{N_{\mathrm{az}},N_{\mathrm{el}}\to\infty}\frac{\rho}{N\mathrm{tr}\left(\Lambda_{\mathrm{s}}\left(\mathbf{H}_{\mathrm{b}}^H\mathbf{H}_{\mathrm{b}}+(\frac{\sigma_{\mathrm{n}}^2KN}{\rho})\mathbf{I}_K\right)^{-1}\mathbf{H}_{\mathrm{b}}^H\mathbf{H}_{\mathrm{b}}\left(\mathbf{H}_{\mathrm{b}}^H\mathbf{H}_{\mathrm{b}}+(\frac{\sigma_{\mathrm{n}}^2KN}{\rho})\mathbf{I}_K\right)^{-1}\right)}\\
&=\lim_{N_{\mathrm{az}},N_{\mathrm{el}}\to\infty}\frac{\rho}{\mathrm{tr}\left(\Lambda_{\mathrm{s}}\left(\frac{\mathbf{H}_{\mathrm{b}}^H\mathbf{H}_{\mathrm{b}}}{N}+(\frac{\sigma_{\mathrm{n}}^2K}{\rho})\mathbf{I}_K\right)^{-1}\frac{\mathbf{H}_{\mathrm{b}}^H\mathbf{H}_{\mathrm{b}}}{N}\left(\frac{\mathbf{H}_{\mathrm{b}}^H\mathbf{H}_{\mathrm{b}}}{N}+(\frac{\sigma_{\mathrm{n}}^2K}{\rho})\mathbf{I}_K\right)^{-1}\right)}\\
&=\frac{\rho}{\mathrm{tr}\left(\Lambda_{\mathrm{s}}\left(\Lambda_{\mathrm{b}}+(\frac{\sigma_{\mathrm{n}}^2K}{\rho})\mathbf{I}_K\right)^{-1}\Lambda_{\mathrm{b}}\left(\Lambda_{\mathrm{b}}+(\frac{\sigma_{\mathrm{n}}^2K}{\rho})\mathbf{I}_K\right)^{-1}\right)}\\
&=\frac{\rho}{\mathrm{tr}\left(\left(\Lambda_{\mathrm{b}}+(\frac{\sigma_{\mathrm{n}}^2K}{\rho})\mathbf{I}_K\right)^{-2}\Lambda_{\mathrm{b}}\Lambda_{\mathrm{s}}\right)}
\end{aligned}
$$

Then, with the limit of $\mathbf{A}$ and α^2, the limit of the sum rate in (12) in the limits of N_{az} and N_{el} can be written as

$$
\begin{aligned}
\tilde{R}&=\lim_{N_{\mathrm{az}},N_{\mathrm{el}}\to\infty}R\\
&=\sum_{k=1}^{K}\log_2\left(1+\frac{\alpha^2\left|\left[\Lambda_{\mathrm{b}}(\Lambda_{\mathrm{b}}+(\sigma_{\mathrm{n}}^2K/\rho)\mathbf{I}_K)^{-1}\right]_{k,k}\right|^2[\Lambda_{\mathrm{s}}]_{k,k}}{\sigma_{\mathrm{n}}^2}\right)\\
&=\sum_{k=1}^{K}\log_2\left(1+\frac{\rho\left|\left[\Lambda_{\mathrm{b}}\left(\Lambda_{\mathrm{b}}+\left(\sigma_{\mathrm{n}}^2K/\rho\right)\mathbf{I}_K\right)^{-1}\right]_{k,k}\right|^2[\Lambda_{\mathrm{s}}]_{k,k}}{\sigma_{\mathrm{n}}^2\mathrm{tr}\left(\left(\Lambda_{\mathrm{b}}+\left(\sigma_{\mathrm{n}}^2K/\rho\right)\mathbf{I}_K\right)^{-2}\Lambda_{\mathrm{b}}\Lambda_{\mathrm{s}}\right)}\right),
\end{aligned}
$$

where the last equation is exactly Eq. (19).

References

1. Sayeed, A., & Brady, J. (2013). Beamspace MIMO for high-dimensional multiuser communication at millimeter-wave frequencies. In *Proceedings of IEEE global communications conference*, pp. 3679–3684.
2. Sayeed, A., & Brady, J. (2014). Beamspace MU-MIMO for high-density gigabit small cell access at millimeter-wave frequencies. In *Proceedings of IEEE 15th international workshop on signal processing advances in wireless communications*, pp. 80–84.
3. Seifi, N., Coldrey, M., & Viberg, M. (2012). Throughput optimization for MISO interference channels via coordinated user-specific tilting. *IEEE Communications Letters*, *16*(8), 1248–1251.
4. Müller, A., Hoydis, J., Couillet, R., & Debbah, M. (2012). Optimal 3D cell planning: A random matrix approach. In *Proceedings of IEEE global communications conference*, pp. 4512–4517.
5. Saur, S., & Halbauer, H. (2011). Exploring the vertical dimension of dynamic beam steering. *2011 8th International workshop on multi-carrier systems and solutions*, pp. 1–5.
6. Friis, H. T. (1946). A note on a simple transmission formula. *Proceedings of the IRE*, *34*(5), 254–256.

Author's personal copy

7. Seifi, N., Coldrey, M., Matthaiou, M., & Viberg, M. (2012). Impact of base station antenna tilt on the performance of network MIMO systems. In Proceedings of IEEE 75th vehicular techenology conference, pp. 1–5.

Anzhong Hu received the B.Eng. degree from Zhejiang University of Technology, Hangzhou, China, in 2009, and the Ph.D. degree from Beijing University of Posts and Telecommunications (BUPT), Beijing,China, in 2014. He is now a lecturer at School of Communication Engineering, Hangzhou Dianzi University. His current research interests include channel estimation and arrayprocessing.